Dalton Transactions

RSC Publishing

PAPER

View Article Online
View Journal | View Issue

Cite this: *Dalton Trans.*, 2013, **42**, 8484

Preparation of potentially porous, chiral organometallic materials through spontaneous resolution of pincer palladium conformers†

Magnus T. Johnson,[a,b] Zoran Džolić,‡[b] Mario Cetina,§[b] Manu Lahtinen,[c] Mårten S. G. Ahlquist,[d] Kari Rissanen,*[b] Lars Öhrström*[e] and Ola F. Wendt*[a]

Understanding the mechanism by which advanced materials assemble is essential for the design of new materials with desired properties. Here, we report a method to form chiral, potentially porous materials through spontaneous resolution of conformers of a PCP pincer palladium complex ({2,6-bis[(di-*t*-butylphosphino)methyl]phenyl}palladium(II)halide). The crystallisation is controlled by weak hydrogen bonding giving rise to chiral qtz-nets and channel structures, as shown by 16 such crystal structures for X = Cl and Br with various solvents like pentane and bromobutane. The fourth ligand (in addition to the pincer ligand) on palladium plays a crucial role; the chloride and the bromide primarily form hexagonal crystals with large 1D channels, whereas the iodide (presumably due to its inferior hydrogen bonding capacity) forms monoclinic crystals without channels. The hexagonal channels are completely hydrophobic and filled with disordered solvent molecules. Upon heating, loss of the solvent occurs and the hexagonal crystals transform into other non-porous polymorphs. Also by introducing a strong acid, the crystallisation process can be directed to a different course, giving several different non-porous polymorphs. In conclusion, a number of rules can be formulated dictating the formation of hexagonal channel structures based on pincer palladium complexes. Such rules are important for a rational design of future self-assembling materials with applications in storage and molecular recognition.

Received 18th January 2013,
Accepted 11th April 2013

DOI: 10.1039/c3dt50190f

www.rsc.org/dalton

Introduction

The design of molecules capable of self-assembling by weak, non-covalent interactions to form well-defined higher-order architectures is an attractive tool for the development of advanced materials with novel properties. Thus, the synthesis and characterisation of molecular-based cages and capsules,[1–7] spheres[8–10] and tubes[11–17] have attracted significant research efforts for the development of new materials and compounds with molecular recognition ability. Of particular interest are inclusion complexes with channels or pores in the crystalline state because of their unique potential capabilities, such as gas storage, ion exchange and catalysis.[18–28]

While it is still difficult to predict trends and principles of the crystallisation process, studies of the relationship between the component molecule and weak non-covalent forces have been carried out with the objective to control self-assembly of molecular building blocks to give well-defined supramolecular architectures in the solid-state. Understanding the nature of these interactions and how to control them systematically can help in the design and synthesis of specific supramolecular synthons for crystal engineering purposes.

It should be noted that the goal of such an assembly is not only channels and other geometrically well-defined objects, but much more general as this is potentially a way of positioning different molecular units vis-à-vis each other in a crystal. Such multi-component crystal engineering, although still a

[a]*Centre for Analysis and Synthesis, Department of Chemistry, Lund University, P.O. Box 124, S-221 00 Lund, Sweden. E-mail: ola.wendt@chem.lu.se*
[b]*Department of Chemistry, Nanoscience Center, University of Jyväskylä, P.O. Box 35, 40014 Jyväskylä, Finland. E-mail: kari.t.rissanen@jyu.fi*
[c]*Department of Chemistry, University of Jyväskylä, P.O. Box 35, 40014 Jyväskylä, Finland*
[d]*Department of Theoretical Chemistry & Biology, School of Biotechnology, KTH Royal Institute of Technology, S-10691 Stockholm, Sweden*
[e]*Department of Chemical and Biological Engineering, Chalmers University of Technology, SE-412 96 Göteborg, Sweden. E-mail: ohrstrom@chalmers.se*

†Electronic supplementary information (ESI) available: Experimental protocols, tables, figures, characterisation data for all new compounds, and X-ray crystallographic data in CIF format. CCDC 913145–913161, 927659–927663. For ESI and crystallographic data in CIF or other electronic format see DOI: 10.1039/c3dt50190f

‡Present address: Ruđer Bošković Institute, Bijenička cesta 54, HR-10000 Zagreb, Croatia.

§Present address: Department of Applied Chemistry, Faculty of Textile Technology, University of Zagreb, Prilaz baruna Filipovića 28a, HR-10000 Zagreb, Croatia.

rare phenomenon,[29] may be advantageous for example in artificial photosynthetic devices.[30] Thus, if the final properties do not depend on covalently linking the parts, it would be advantageous to let a multi-component system self-assemble in a way that creates the desired relation between all the molecules, and this can only be done with a detailed knowledge of intermolecular interactions and the use of supramolecular synthons of different types.

The importance of polymorphs and pseudo-polymorphs should be emphasised in the quest to obtain this knowledge. Not only are these, in their own respect, important for pharmaceutical applications,[31] but the fact that we, in the case of true polymorphs, vary only the crystal structure, and not the components, makes these ideal for the study of intermolecular interactions in the solid state.

Recently, we have demonstrated the influence of weak hydrogen bonding interactions on the solid state structures of various palladium(II) (PCPPd) complexes (**1–3**),[32] Chart 1.

The varied nature and geometry of the intermolecular interactions of the structures in these organometallic complexes give rise to a range of different supramolecular architectures: from strongly hydrogen-bonded dimers of **1**, over weakly hydrogen-bonded zig-zag chains in **2** to a 3D quartz net (the chiral qtz topology[33]) with hydrophobic chiral channels in **3**. In view of the interesting properties of **3** and its potential in the field of porous materials we have investigated the possibilities of channel formation with similar pincer complexes containing terminal metal halides **4–6**. These complexes and others alike are well known in the literature as precursors to further functionalised complexes in, for example, catalysis, bond activation, sensors and switches.[34–40] Recently, they were also shown to be excellent halogen bond acceptors.[41]

Here we demonstrate the excellent capability of PCPPdCl complex **4** and PCPPdBr complex **5** for the formation of chiral, porous structures by non-covalent interactions. We also explore the wide possibilities of polymorphs and pseudo-polymorphs for these systems by the solvent, pH and temperature effect on the crystallisation process. The effect of the halogen atom and other factors affecting crystal packing is thoroughly investigated together with composition and stability studies.

Results and discussion

Channel compounds: solvates of 4 and 5

Compound **4** was prepared as described in the literature.[36] When recrystallised from pentane, unit cell analysis by X-ray diffraction showed that this compound does not, at least in our hands and to any measurable extent, crystallise in the orthorhombic space group $P2_12_12_1$ as reported previously (CSD Refcode: AGEWOY[42]). Although pentane was used in both cases, we could not successfully repeat the orthorhombic crystallisation under seemingly identical conditions. Instead, as shown in Fig. 1, **4** (denoted as **4**·Pen when crystallised from pentane) crystallised as a conglomerate in either of the two enantiomorphic, hexagonal space groups $P6_122$ and $P6_522$. Similarly to **3**, these structures contain a hexagonal channel along the *c*-axis as shown in Fig. 2. As the walls of the channel are covered by *tert*-butyl (*t*Bu) groups, they form a completely hydrophobic environment, filled with disordered solvent molecules. The dimension of the channels (excluding solvent) formed along the *c*-axis is approximately 7 Å in diameter, taking into account the van der Waals radii of the surface atoms, thus having the dimensions of a microporous material as defined by IUPAC.[43] In accordance with the space group symmetry, a view along the *c*-axis shows the molecules displaced in a honeycomb fashion, thereby forming hexagons around the channels. The total potential solvent accessible void is 714 Å^3, corresponding to 16.0% of the unit cell volume, as calculated by *PLATON*[44] (Table S1†).

As shown by the large and diffuse residual electron density, the solvent molecules occupying the channels are highly disordered. Although not on a molecular level, the residual electron density could be modelled and refined isotropically as a long chain stretching through the centre of the channels along the *c*-axis, as was previously demonstrated for **3**.[32] Attempts to recrystallise **4** in the presence of various haloalkanes and arenes repeatedly resulted in the same structure, having

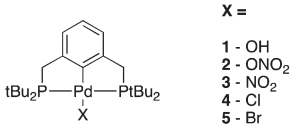

X =

1 - OH
2 - ONO_2
3 - NO_2
4 - Cl
5 - Br
6 - I

Chart 1

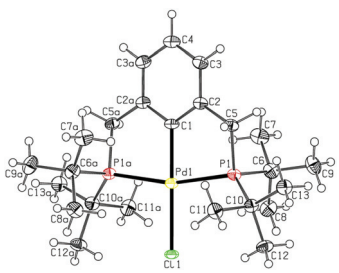

Fig. 1 The molecular structure of **4**·Pen, with the atom-numbering scheme. Displacement ellipsoids for non-hydrogen atoms are drawn at the 40% probability level.

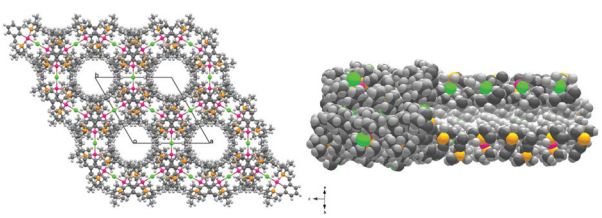

Fig. 2 Crystal packing diagrams of **4**·Pen. Left: viewed along the *c*-axis, showing channels orthogonal to the *a* and *b* axes; Right: view of a cut open channel showing its hydrophobic inner surface (solvent has been removed for clarity).

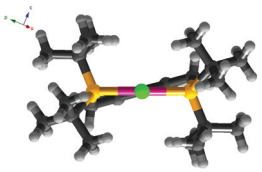

Fig. 3 The origin of chirality in **3–5** solvates, the dihedral angle (P1–C2–C2a–P1a), 27.88° for **3** (NO_2), 27.92° for **4** (Cl) and 27.14° for Br (**5**).

disordered solvent molecules in the channels, although the final electron density was obviously higher when solvents with heavier elements (higher electron count) were used, *cf.*, Table S1.†

As can be seen in Fig. 3, the phenyl rings in the complexes are always slightly twisted compared to the coordination plane, thereby giving chiral molecules in the solid state. Hence, the molecule lacks a mirror plane but instead has a C2 axis relating the two sides of the molecule. The sense of chirality is the same in each crystal, giving rise to axially chiral crystals, as manifested by the chirodescriptive[45] space group. The sense of chirality can also be described by the dihedral angle (P1–C2–C2a–P1a, see Fig. 1) that was shown to vary in a very short range (from |25|° to |28|°) in all the structures (ESI, Table S1†). Depending on the space group ($P6_122$ or $P6_522$) the angles have opposite signs.

In solution, the molecular structure **4** is achiral since the interconversion between the two chiral conformations is presumably very fast. To estimate the barrier of the interconversion between the two conformers (wherein one of the *t*Bu-groups on each phosphine is switched from axial to equatorial and the other *t*Bu-group *vice versa*), we performed a scan of the dihedral angle P–Pd–C1–C2 using DFT (B3LYP/LACVP)[46] (*cf.* Fig. 4). This leads to the formation of the configuration where the *t*Bu-groups on the two phosphines point in the same direction, *i.e.*, both *t*Bu-groups below the square plane are equatorial and both above are axial. The scan indicates that the energy required, as expected, is very low at 3.2 kcal mol^{-1} indicating that the switching process is very rapid, indeed. Consequently this excludes the possibility that the complex is "locked" in one conformation in solution and the interconversion is too fast to be studied by NMR spectroscopy.

Instead it is reasonable to assume that the formation of the axial chirality forces the molecules to crystallise in a single conformation resulting in the two enantiomorphs. This is then not equal but equivalent to what in the context of enantiomeric molecular species is called spontaneous resolution.

PCPPdBr **5** behaves similarly to **4** by forming isomorphous hexagonal channel structures when recrystallised from many common organic solvents such as alkanes, bromoalkanes and ethanol (*cf.* ESI, Table S2†). As for **4**, crystallisation occurs in either of the enantiomorphic space groups $P6_122$ and $P6_522$.

Although the absolute total potential solvent accessible volume is larger in **5**·solvates than in **4**·solvates, the relative potential solvent volume is approximately the same, 16%. The diameter of the channels in both structures is approximately 7 Å. Just as was noted for **4**, the hexagonal structures are obtained not only from non-polar linear alkanes, but also from, *e.g.*, ethanol, cyclohexane and halogenated solvents.

There are only two significant intermolecular contacts in solvated **4** and **5** (Fig. 5): methyl–methyl interactions with closest H···H distances of 2.54 and 2.60 Å in solvates of **4** and **5**, respectively (C···C = 3.45 Å in **4**, 3.50 Å in **5**) and the halogen···H–C–P contacts which are tabulated in Table 1. We

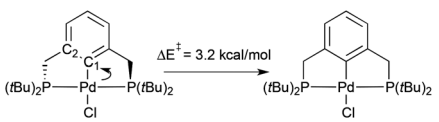

Fig. 4 Conversion between the conformations is calculated by DFT to have a low barrier, 3.2 kcal mol^{-1}. Note that the structure to the right has a P–Pd–C1–C2 dihedral angle of 0°.

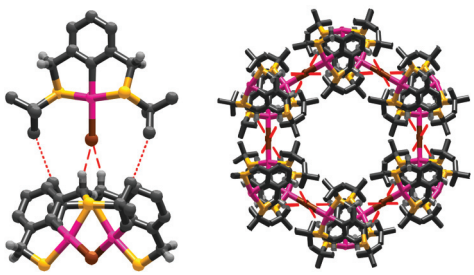

Fig. 5 Left: Part of the crystal structure of **5**·Hex-1 showing the only significant intermolecular interactions, the HCH···Br contacts as dashed lines and methyl–methyl contacts as dotted lines; Right: Crystal packing viewed along the *c*-axis, showing channel formation at the intersection of the *a* and *b* axes with only the Br···H interactions displayed. In both pictures only H5 hydrogens are shown.

Table 1 Some intermolecular interactions in **3–5** and the highest frequency occurrence of corresponding interactions found in the Cambridge Crystallographic Database

		Dist. **A**···H–C		Angle A···H–C		
Comp.	Interaction	Meas.	CSD	Meas.	CSD	Pd···Pd [Å]
3[a]	ONO···H–C	3.28(1) Å	3.4 Å[c]	141.3(3)°	128°	9.247(1)
4[b]	Cl···H–C	3.769(4) Å	3.8 Å[d]	132.3(2)°	124°	9.1148(5)
5[b]	Br···H–C	3.744(7) Å	3.9 Å[d]	131.5(5)°	124°	9.1753(8)

[a] Measurements reported at 293 K. [b] Measurements made at 123 K. [c] Transition metal-(NO_2)···H–C structures were retrieved to obtain better statistics. [d] Pd–Cl and Pd–Br structures were retrieved.

propose that those non-classical hydrogen bonds residing between the halogens (or nitro group in **3**) and the slightly acidic methylene bridge are the foundation for the formation of channel structures, as the described interactions lead to a four-connected three-dimensional chiral net with **qtz**-topology.

In other examples, like in complexes **1** and **2**, the small anionic ligand is clearly essential for controlling the molecular packing, whereas in the methyl derivative, PCPPdMe,[35] the overall motif resembles close packing with no channel formation. We therefore cannot assign any structure-directing role to the methyl–methyl close contacts, albeit no doubt they have some importance for the global stability of the crystal. Whether this is of smaller or greater importance than the dispersion interaction between the hydrophobic channel and the solvent molecules is impossible to judge.

Unlike PCPPdCl **4** and PCPPdBr **5**, recrystallisation of PCPPdI **6** from the above listed solvents neither resulted in hexagonal nor solvated structures.

Compound **6** will be further discussed in the polymorphism section, but for now we can conclude that just as we have previously noted in the formation of halogen bonds, the bromide strikes the best balance between being sterically accessible and a good hydrogen (halogen) bond acceptor. It can also be noted that the use of hydrogen bonding solvents such as ethanol is not sufficient to prevent the channel formation but under strongly acidic conditions (*vide infra*) the hydrogen bond patterns in the channels are apparently broken up and other polymorphs are formed preferentially.

The network structure of **3** has already been described in detail,[32] and this interpretation applies also to the solvates of **4** and **5** (see Fig. 6), but a few additional, new issues need to be addressed here.

This type of network analysis[47] is a very general tool for describing and understanding crystal structures, and goes back to the seminal work of Wells.[48] For instance in the present solvated structures, it is easy to focus on the channels only, and to discover their "double helical" nature. Indeed, if the **qtz**-net is cut to leave the six-fold channels alone, two disconnected helices are found, but as these are integer parts of the complete network, such an analysis gives none but a fragmented picture of the structure.

The second point we wish to make concerns the chirality and the spontaneous resolution of chiral conformers. There is no rule that prevents molecules of the same chirality from assembling into a non-chiral net, for example in this case the diamond or **dia**-net, but for the solvates **3–5** the resolution of the chiral conformers was always accompanied by the formation of the chiral quartz-net. Recently, we have found a number of examples where conglomerate formation from racemic solutions of regular enantiomers also has resulted in hydrogen-bonded nets with inherent chirality, just like the **qtz**-net,[49–50] and have hypothesised that one possible mechanism for conglomerate formation is that the building blocks and their supramolecular synthons have the right geometry for the formation of one of the chiral nets.

For an extended study of the channel content and their properties, compound **5** was chosen since large high quality crystals were conveniently obtained by slow evaporation in time intervals ranging from 24 to 48 hours. Under the same conditions, the formation of large high quality crystals of **4** typically required several weeks. This may be explained by the relatively shorter H···X contact in **5** and that the size of the bromide matches the palladium atom better and thus facilitates packing by having an overall higher lattice enthalpy. This also matches the theory that hydrogen bonds are the structure directing factor, as does the fact that the Pd···Pd distances match the differences in the size of the anionic ligand.

While the TGA measurements (*vide infra*) are completely consistent with the channels and their proposed contents, these properties are better discussed in the context of the many different polymorphs formed in these systems, so we now turn to the second part of this study.

Polymorphism of 4–6

As mentioned earlier, recrystallisation of PCPPdI **6** afforded only non-helical and -solvated structures and despite the attempted use of many different solvents, crystals were only obtained from methanol and heptane. PCPPdI **6** crystallises in the monoclinic space group $P2_1/c$ and the molecules are linked by C–H···π interactions into chains. There is also one short contact occurring between the methyl group hydrogen atom and the C5 atom of the phenyl ring in the neighbouring molecule [H20B···C5 = 2.83 Å].

The significant difference of **6** compared to **4** and **5** may partly be explained by the fact that the iodine atom is substantially larger than the bromine and chlorine, although the main reason is most probably the weaker hydrogen bond acceptor capability of iodine. As seen in Fig. 7 there is no drastic change in the steric properties of the three compounds.

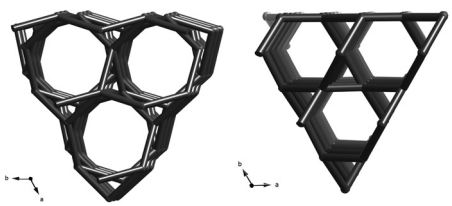

Fig. 6 Quarts (**qtz**) nets formed by the weak hydrogen bonds in **5** (left; in **4** the net is very similar) and the ideal (most symmetric) form of the **qtz**-net (right). Each link connects two four-connected Pd atoms. All other atoms are hidden.

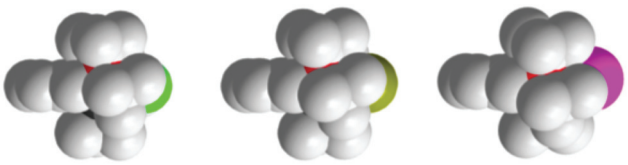

Fig. 7 PCPPdCl **4**, PCPPdBr **5**, and PCPPdI **6**, viewed from the side in the plane of the aromatic ring in spacefill models. Hydrogens are omitted for clarity.

Initial attempts to investigate halogen bonding properties of **5** using elemental bromine led to the successful crystallisation of a non-solvated orthorhombic crystal structure in space group *Fd2d* with calculated density 1.456 g cm^{-3} ($\mathbf{5}_{oF}$). A possible explanation may be that the residual water existing in the technical grade solvents used was sufficient to form a small amount of hydrobromic acid, which in turn affected the crystallisation process. In order to test this hypothesis, we added concentrated HBr to **5** in a separate experiment. In this way an orthorhombic non-solvated structure was obtained as a second polymorph $\mathbf{5}_{oP}$ in space group *Pbca* with a calculated density of 1.431 g cm^{-3} (Fig. S2†). Structure $\mathbf{5}_{oF}$ contains no solvent accessible voids and there are no C–H···π interactions or short contacts. The high symmetry in this structure is partially manifested by the phenyl rings being parallel to the *b*-axis, as can be seen in Fig. 8.

Compared to $\mathbf{5}_{oF}$, the structure of $\mathbf{5}_{oP}$ shows a lower density, and one shorter H···Br contact (Table S4†). Thus, the molecules of $\mathbf{5}_{oP}$ are linked by C10–H10A···Br1 hydrogen bond into chains parallel to the *b*-axis (Fig. 9). In addition, one short intermolecular contact of 2.81 Å, H8A···C10, is also found in this structure. The P1–C2–C6–P2 dihedral angle in $\mathbf{5}_{oP}$ is approximately equal to those observed in the hexagonal structures of **4** and **5** and 7° larger than in $\mathbf{5}_{oF}$.

We note that although the methyl derivative also crystallises in space group *Pbca*,[35] it is not isostructural to $\mathbf{5}_{oP}$. Instead, $\mathbf{5}_{oP}$ is closely related to the hydrogen carbonate derivative with unit cell parameters 15.7850(3) Å, 16.3154(4) Å, and 21.8306(3) Å,[51] compared to 15.3928(4) Å, 15.5649(4) Å, and 22.4687(6) Å for $\mathbf{5}_{oP}$.

Yet another polymorph of **5** was obtained after the variable temperature powder diffraction experiment presented in the next section. A sample of crude **5** had then been heated in several stages up to 240 °C and after cooling, colourless plate-like crystals were collected from the sample cavity. A single crystal structure determination revealed a new monoclinic PCPPdBr polymorph ($\mathbf{5}_{m}$). Two independent molecules of $\mathbf{5}_{m}$ (designated as A and B) are linked by C–H···Br hydrogen bond into dimers (Table S4 and Fig. S4†), in contrast to $\mathbf{5}_{oP}$ where the molecules form infinite chains. The hydrogen-bonded dimers are weakly linked with adjacent molecules by two C–H···π interactions accomplished between *t*Bu-group atoms and the phenyl rings of two A and two B molecules. Both phenyl rings of two independent molecules form an angle of 23.4(2)°, *i.e.*, they are virtually parallel. It is also clear that the P–C–C–P dihedral angle in molecule B differs significantly from that obtained for A, as well as from the angles obtained for the other PCPPd complexes (Table S3†).

Most likely this is the thermodynamic product as it was obtained at high temperature and also has the highest calculated density, 1.466 g cm^{-3}.

As the role of the acid in the crystallisation process became clear, the same method was applied to PCPPdCl **4**. After the addition of 3 M hydrochloric acid to an ethanol solution of **4**, a monoclinic $P2_1/c$ ($\mathbf{4}_{m}$) structure was obtained. With conc. HCl, an orthorhombic polymorph ($\mathbf{4}_{o}$) crystallised in $P2_12_12_1$ (Fig. S3†), equivalent to the previously published structure.[42] Structure $\mathbf{4}_{o}$ display C–H···Cl interactions organising the complex into chains parallel to the *b*-axis (Fig. 10a), while the same type of interaction in $\mathbf{4}_{m}$ forms chains parallel to the *c*-axis (Fig. 10b). Besides C–H···Cl interactions, two additional short H···C contacts in $\mathbf{4}_{m}$ are also present. The P1–C2–C5–P2 dihedral angle in $\mathbf{4}_{m}$ and $\mathbf{4}_{o}$ differs by 3°.

The intramolecular bond lengths in all PCPPdBr and PCPPdCl polymorphs, as well as in the previously reported orthorhombic polymorph of PCPPdCl, are within 3σ values. The exception is the Pd–Cl bond distance in $\mathbf{4}_{o}$ which is 0.025 Å longer [2.4224(9) Å] compared to $\mathbf{4}_{m}$ [2.3976(4) Å] and the previously reported structure [2.397(7) Å]. The same is true for the Pd–C bond in $\mathbf{5}_{oF}$ [2.052(9) Å] which is 0.028 Å longer than the corresponding one in $\mathbf{5}_{oP}$ [2.024(4) Å].

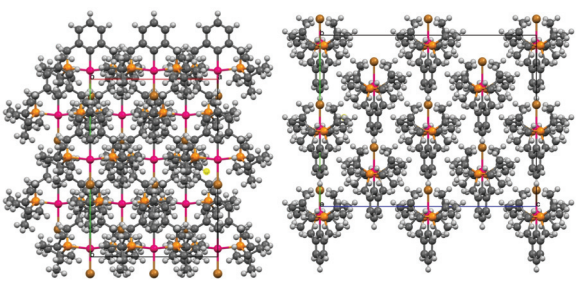

Fig. 8 Crystal packing diagrams of $\mathbf{5}_{oF}$, showing the arrangement of the molecules in the unit cell. Left: viewed along the *c*-axis; Right: viewed along the *a*-axis.

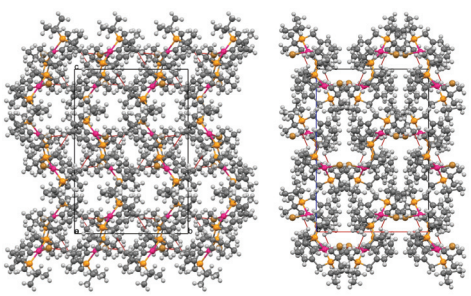

Fig. 9 Crystal packing diagrams of $\mathbf{5}_{oP}$, showing the arrangement of the molecules in the unit cell. Left: viewed along the *a*-axis; Right: viewed along the *b*-axis.

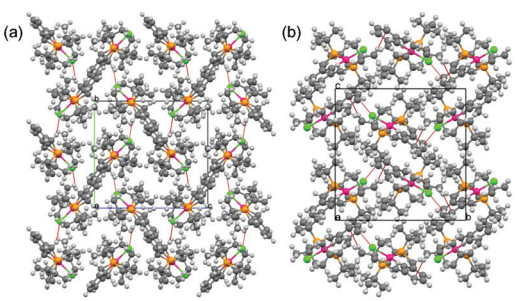

Fig. 10 Crystal packing diagrams along the *a*-axis, showing C–H···Cl hydrogen bonding chains of: (a) $\mathbf{4}_{o}$ parallel to the *b*-axis; (b) $\mathbf{4}_{m}$ parallel to the *c*-axis.

XRD and TGA studies

To gain more information about the bulk properties of the PCPPd complexes, X-ray powder diffraction (XRD) data for complexes **4**, **5**, **5**·BuBr solvate and **6** were acquired. The resulting diffraction data are depicted in Fig. 11 and 12 with the simulated XRD patterns corresponding to the single crystal structures of PCPPd halides (Cl, Br and I, respectively) $\mathbf{4}_{o,sim}$, $\mathbf{4}_{m,sim}$, **4**·Pen_{sim}, $\mathbf{5}_{oF,sim}$, $\mathbf{5}_{oP,sim}$, $\mathbf{5}_{m,sim}$, **5**·$BuBr_{sim}$, **5**·Hex_{sim} and $\mathbf{6}_{m,sim}$. In addition to the conventional XRD patterns, a series of diffraction patterns were measured for complex **5** using variable temperature XRD, as can be seen in Fig. 13.

The PCPPdCl bulk powder **4** (Fig. 11) proved to be a mixture of crystalline phases. One of the phases is consistent with monoclinic PCPPdCl ($P2_1/c$) $\mathbf{4}_{m,sim}$, whereas the diffraction peaks of the second, seemingly dominant, phase resemble the simulated XRD pattern of the hexagonal **4**·Pen_{sim}, although the bulk powder was not crystallised from pentane but from benzene. Moreover, the experimental pattern contains some peaks that belong to a third, unknown structure form.

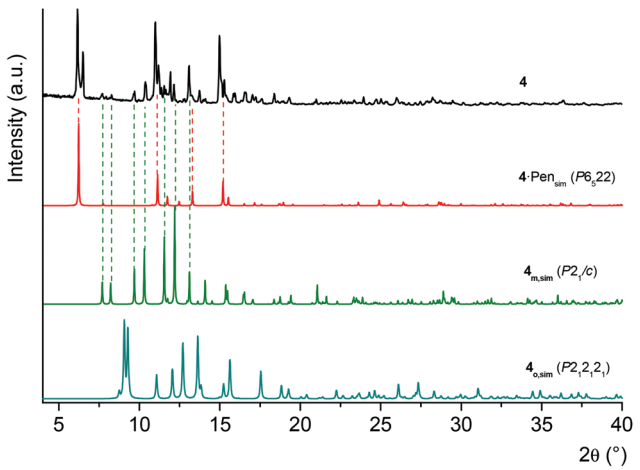

Fig. 11 Experimental XRD pattern of **4** compared with simulated patterns of **4**·Pen_{sim}, $\mathbf{4}_{m,sim}$ and $\mathbf{4}_{o,sim}$.

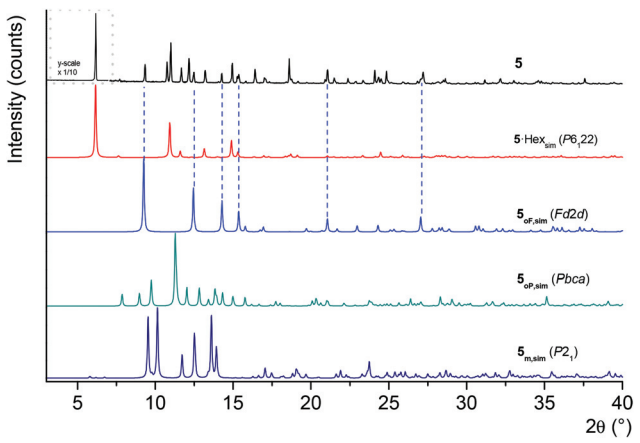

Fig. 12 Experimental XRD pattern of **5** compared with simulated patterns of **5**·Hex_{sim}, $\mathbf{5}_{oF,sim}$, $\mathbf{5}_{oP,sim}$ and $\mathbf{5}_{m,sim}$. The 2θ-range from 4 to 7° in the pattern of **5** is shown in different scales due to a very strong reflection.

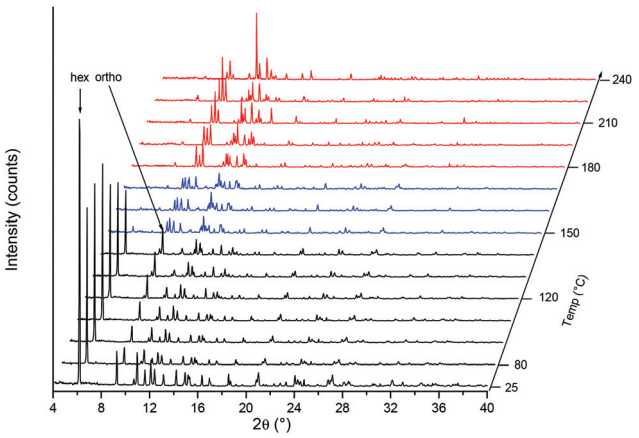

Fig. 13 Variable temperature XRD patterns of **5** heated from RT to 240 °C under the air atmosphere. The strongest peaks of the hexagonal channel and orthorhombic non-solvated bromide structures are marked in the graph.

The experimental XRD pattern of the bulk powder of **5** was compared with the simulated patterns $\mathbf{5}_{oF,sim}$, $\mathbf{5}_{oP,sim}$, $\mathbf{5}_{m,sim}$ and **5**·Hex_{sim} (structure analogue with **5**·BuBr). Indeed, the experimental pattern is in good agreement with the simulated patterns of **5**·Hex and **5**·$BuBr_{sim}$ (Fig. 12). Also a few weaker diffraction peaks *e.g.* at 2θ-angles of 9.3°, 12.5° and 14.2° can be observed in the XRD pattern, indicating that the bulk powder contains also orthorhombic $\mathbf{5}_{oF,sim}$ as a minor component. The above observations strongly suggest that, as expected, the bulk powder of **5** is mainly in the hexagonal crystal system thus having a channel structure. The channels are most likely filled with hexane solvent used for crystallisation.

In the case of PCPPdI **6**, the bulk powder and single crystals are structurally identical as the experimental and the simulated ($\mathbf{6}_{m,sim}$) patterns are consistent with each other (Fig. S5†).

In order to monitor the temperature dependent changes of the channel structures variable temperature XRD analyses were carried out with complex **5** (Fig. 13). The series of XRD patterns reveal a gradual degradation of the hexagonal structure form between 120 and 150 °C. At 120 °C the diffraction pattern of the channel structure remains relatively unchanged, but already the first pattern taken at 150 °C shows dramatic changes, as nearly all diffraction peaks of the hexagonal form have either weakened substantially or disappeared completely, similarly as are the peaks originating from the face-centred orthorhombic form $\mathbf{5}_{oF}$. At the same time, a number of new peaks can be observed in the XRD pattern *e.g.* in the 2θ-range of 9 to 10° and 11 to 14°. These peaks can be assigned to the new monoclinic structure modification PCPPdBr $\mathbf{5}_{m}$, the crystal structure of which was determined later from the crystals that were formed as a result of this experiment. The structural change from the hexagonal to the primitive orthorhombic form (+ an unidentified form) gets more evident with an increase of temperature, and the solvent free structure modifications ($\mathbf{5}_{m}$ + an unidentified form) are the only phases left at temperatures above 180 °C.

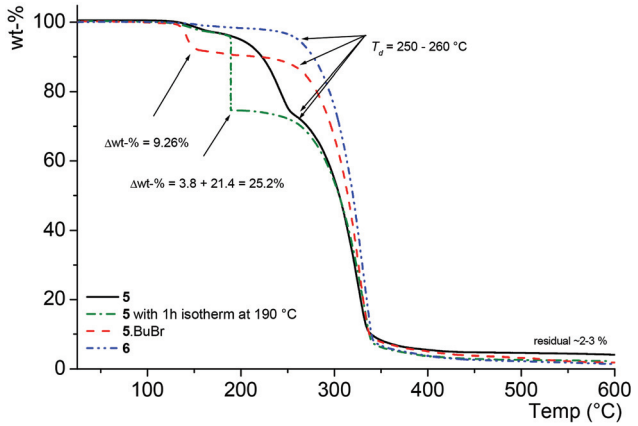

Fig. 14 TG curves of **5**, **5**·BuBr and **6** measured under a nitrogen atmosphere with a heating rate of 10 °C min^{-1}.

The thermal properties were further examined for complexes **5**, **5**·BuBr and **6** with a thermogravimetric analyser. The potential influence of oxidative conditions (air) was tested by measuring a few TG curves of complex **5** both under flowing air and N_2 atmospheres. As a result, no significant differences were found between the atmospheres but as a precaution the samples were analysed under an N_2 atmosphere in further studies. TG curves of bromide complexes **5** and **5**·BuBr show weight loss with a clearly observable initiation temperature ranging between 135 and 140 °C. In contrast, only a slow gradual weight loss of <2 wt% from ~100 to 250 °C is observed for iodide complex **6** prior to its decomposition above 260 °C (Fig. 14 and Table S5†). For **5**·BuBr, the weight loss can be assigned to the disappearance of *n*-bromobutane which occurs in a temperature range of 133–160 °C, followed by a constant stage and eventually onset of thermal decomposition above 250–260 °C. The observed weight loss of desolvation (Δwt% = 9.26%) corresponds to about 0.42 mole of *n*-BuBr/Pd in **5**·BuBr solvate. For **5** the corresponding weight loss between 135 and 190 °C under constant heating (Δwt% = ~3.3%) is significantly smaller, thereby corresponding to a loss of 0.23 moles of hexane that is trapped in the channels. The second major weight loss of about 25% occurs between 190 and 250 °C. As this weight loss is too large to originate from hexane release due to mismatching stoichiometry, an additional TG analysis was made for **5** using an isothermal step (an hour at 190 °C) in the heating profile. As a result, a similar weight loss (Δwt% = 25.2%) occurred already at 190 °C, which is followed by major degradation above 250 °C. Again, as the weight loss cannot be attributed to solvent loss due to mismatching stoichiometry, and on the other hand the temperature-dependent XRD analysis indicated that the complex **5** is thermally stable until around 240 °C, it is assumed that partial sublimation of the complex occurs between ~190 and 250 °C. This assumption is further supported by the residual weight (~3 wt%) found at 600 °C, which is significantly less than would be expected if Pd and/or PdO based compounds are the annealing products. In conclusion, the hexagonal channels release their solvent contents between 130 and 190 degrees but as judged from the XRD this coincides with major rearrangements to other polymorphs. One of these polymorphs was detected by the variable temperature XRD experiment as several large colourless plate-like crystals of $\mathbf{5}_m$, which had formed inside the sample cavity. The observation of this phase clearly suggests that at least PCPPdBr can remain stable at relatively high temperatures. A similar behaviour is anticipated for the iodide complex based on the TG analysis, as similar TG curve profiles onset temperatures of 255–263 °C for the decomposition as well as residual weights were determined for both complexes **5** and **6** (Table S5†).

Conclusions

This work demonstrates a method to produce chiral, potentially porous materials through spontaneous resolution of PCP-Pd pincer complexes. Furthermore, this demonstrates how weak hydrogen bond supramolecular synthons can be used to consistently form desired enantiopure network compounds with large channels by resolving chiral conformers through the formation of a chiral net topology. It also shows the limitations of this approach in terms of which exact synthons can be used (NO_2^-, Cl^-, $Br^-\cdots$H–C) and where it fails ($I^-\cdots$H–C). Furthermore, another limitation is revealed to be the lability of the formed structures, demonstrated through the many polymorphs detected. Some guidelines on the predictibility of hexagonal crystallisation with aromatic PCP-Pd complexes could then be summarised as follows: (1) The X-ligand should be aprotic. (2) The X-ligand has to be of sufficient size to reach out of the steric bulk posed by the *tert*-butyl ligands, although it must not be too large to significantly affect the packing. (3) The X-ligand should be a bidendate HB acceptor. (4) When the X-ligand is polyatomic, the HB acceptor atoms must manifest periplanar hydrogen bonding.

Acknowledgements

We thank the Academy of Finland (KR: proj. no. 130629, 122350, 140718), the Swedish Research Council (OFW, LÖ) and the Knut and Alice Wallenberg foundation for financial support. This work was in part supported by Nordforsk *via* the Nordic–Baltic Network in Crystal Engineering and Supramolecular Materials.

Notes and references

1 D. L. Caulder and K. N. Raymond, *Acc. Chem. Res.*, 1999, **32**, 975–982.
2 M. Fujita, M. Tominaga, A. Hori and B. Therrien, *Acc. Chem. Res.*, 2005, **38**, 369–378.
3 P. Mal, D. Schultz, K. Beyeh, K. Rissanen and J. R. Nitschke, *Angew. Chem., Int. Ed.*, 2008, **47**, 8297–8301.
4 M. Yoshizawa, J. K. Klosterman and M. Fujita, *Angew. Chem., Int. Ed.*, 2009, **48**, 3418–3438.

5 S. Leininger, B. Olenyuk and P. J. Stang, *Chem. Rev.*, 2000, **100**, 853–907.
6 D. J. Cram, *Container molecules and their guests*, Royal Society of Chemistry, London, 1994.
7 P. Mal, B. Breiner, K. Rissanen and J. R. Nitschke, *Science*, 2009, **324**, 1697–1699.
8 H. Masu, K. Katagiri, T. Kato, H. Kagechika, M. Tominaga and I. Azumaya, *J. Org. Chem.*, 2008, **73**, 5143–5146.
9 K. Suzuki, M. Kawano, S. Sato and M. Fujita, *J. Am. Chem. Soc.*, 2007, **129**, 10652–10653.
10 L. T. Scott, M. M. Boorum, B. J. McMahon, S. Hagen, J. Mack, J. Blank, H. Wegner and A. de Meijere, *Science*, 2002, **295**, 1500–1503.
11 T. Iwanaga, R. Nakamoto, M. Yasutake, H. Takemura, K. Sako and T. Shinmyozu, *Angew. Chem., Int. Ed.*, 2006, **45**, 3643–3647.
12 H. Mansikkamäki, M. Nissinen and K. Rissanen, *Angew. Chem., Int. Ed.*, 2004, **43**, 1243–1246.
13 W. P. Liao, Y. L. Li, X. F. Wang, Y. F. Bi, Z. M. Su and H. J. Zhang, *Chem. Commun.*, 2009, 1861–1863.
14 H. Mansikkamäki, S. Busi, M. Nissinen, A. Ahman and K. Rissanen, *Chem.–Eur. J.*, 2006, **12**, 4289–4296.
15 V. G. Organo, V. Sgarlata, F. Firouzbakht and D. M. Rudkevich, *Chem.–Eur. J.*, 2007, **13**, 4014–4023.
16 T. Kaczorowski, I. Justyniak, T. Lipinska, J. Lipkowski and J. Lewinski, *J. Am. Chem. Soc.*, 2009, **131**, 5393–5395.
17 G. R. Desiraju, *Nature*, 2001, **412**, 397–400.
18 G. Ferey, C. Mellot-Draznieks, C. Serre and F. Millange, *Acc. Chem. Res.*, 2005, **38**, 217–225.
19 N. W. Ockwig, O. Delgado-Friedrichs, M. O'Keeffe and O. M. Yaghi, *Acc. Chem. Res.*, 2005, **38**, 176–182.
20 J. Tian, P. K. Thallapally, S. J. Dalgarno, P. B. McGrail and J. L. Atwood, *Angew. Chem., Int. Ed.*, 2009, **48**, 5492–5495.
21 A. Comotti, S. Bracco, G. Distefano and P. Sozzani, *Chem. Commun.*, 2009, 284–286.
22 T. D. Nixon, L. D. Dingwall, J. M. Lynam and A. C. Whitwood, *Chem. Commun.*, 2009, 2890–2892.
23 C. H. Gørbitz, *Chem.–Eur. J.*, 2007, **13**, 1022–1031.
24 G. Z. Yuan, C. F. Zhu, W. M. Xuan and Y. Cui, *Chem.–Eur. J.*, 2009, **15**, 6428–6434.
25 P. Dechambenoit, S. Ferlay, N. Kyritsakas and M. W. Hosseini, *J. Am. Chem. Soc.*, 2008, **130**, 17106–17113.
26 J. L. Atwood, L. J. Barbour and A. Jerga, *Science*, 2002, **296**, 2367–2369.
27 M. Albrecht, M. Lutz, A. L. Spek and G. van Koten, *Nature*, 2000, **406**, 970–974.
28 Z. Huang, P. S. White and M. Brookhart, *Nature*, 2010, **465**, 598–601.
29 M. Ghazzali, V. Langer, K. Larsson and L. Öhrström, *CrystEngComm*, 2011, **13**, 5813–5817, and references therein.
30 M. R. Wasielewski, *Acc. Chem. Res.*, 2009, **42**, 1910–1921.
31 P. Vishweshwar, J. A. McMahon, J. A. Bis and M. J. Zaworotko, *J. Pharm. Sci.*, 2006, **95**, 499–516.
32 R. Johansson, L. Öhrström and O. F. Wendt, *Cryst. Growth Des.*, 2007, **7**, 1974–1979.
33 M. O'Keeffe, M. A. Peskov, S. J. Ramsden and O. M. Yaghi, *Acc. Chem. Res.*, 2008, **41**, 1782–1789.
34 M. Albrecht and G. van Koten, *Angew. Chem., Int. Ed.*, 2001, **40**, 3750–3781.
35 R. Johansson, M. Jarenmark and O. F. Wendt, *Organometallics*, 2005, **24**, 4500–4502.
36 R. Johansson and O. F. Wendt, *Dalton Trans.*, 2007, 488–492.
37 M. T. Johnson, R. Johansson, M. V. Kondrashov, G. Steyl, M. S. G. Ahlquist, A. Roodt and O. F. Wendt, *Organometallics*, 2010, **29**, 3521–3529.
38 D. Morales-Morales and C. M. Jensen, *The chemistry of pincer compounds*, Elsevier, Amsterdam, Boston, 1st edn, 2007.
39 J. T. Singleton, *Tetrahedron*, 2003, **59**, 1837–1857.
40 M. E. van der Boom and D. Milstein, *Chem. Rev.*, 2003, **103**, 1759–1792.
41 M. T. Johnson, Z. Dzolic, M. Cetina, O. F. Wendt, L. Öhrström and K. Rissanen, *Cryst. Growth Des.*, 2012, **12**, 362–368.
42 B. F. M. Kimmich, W. J. Marshall, P. J. Fagan, E. Hauptman and R. M. Bullock, *Inorg. Chim. Acta*, 2002, **330**, 52–58.
43 J. Rouquerol, D. Avnir, C. W. Fairbridge, D. H. Everett, J. H. Haynes, N. Pernicone, J. D. F. Ramsay, K. S. W. Sing and K. K. Unger, *Pure Appl. Chem.*, 1994, **66**, 1739–1758.
44 A. L. Spek, *J. Appl. Crystallogr.*, 2003, **36**, 7–13.
45 C. J. Wallentin, E. Orentas, K. Wärnmark and O. F. Wendt, *Z. Kristallogr.*, 2009, **224**, 607–608.
46 The calculations were performed using the Jaguar 7.6 program package by Schrödinger LLC.
47 L. Öhrström, in *Encyclopedia of supramolecular chemistry*, ed. L. Barbour, John Wiley & Sons, Chichester, UK, 2012, vol. 8. Supramolecular materials chemistry, and reference therein.
48 A. F. Wells, *Three-dimensional nets and polyhedra*, Wiley, New York, 1977.
49 C. J. Wallentin, E. Orentas, M. T. Johnson, N. B. Bathori, E. Butkus, O. F. Wendt, K. Wärnmark and L. Öhrström, *CrystEngComm*, 2012, **14**, 178–187.
50 C. J. Wallentin, E. Orentas, M. T. Johnson, E. Butkus, O. F. Wendt, L. Öhrström and K. Wärnmark, *CrystEngComm*, 2009, **11**, 1837–1841.
51 R. Johansson and O. F. Wendt, *Organometallics*, 2007, **26**, 2426–2430.